Biochimica et Biophysica Acta, 1028 (1990) 95–102
Elsevier

BBAMEM 74978

Proton flow along lipid bilayer surfaces: effect of halothane on the lateral surface conductance and membrane hydration

Tadayoshi Yoshida [1], Keijiro Taga [1], Hirofumi Okabayashi [1], Hiroshi Kamaya [2] and Issaku Ueda [2]

[1] *Department of Applied Chemistry, Nagoya Institute of Technology, Showa-Ku, Nagoya (Japan) and* [2] *Anesthesia Service, VA Medical Center, Salt Lake City, UT (U.S.A.)*

(Received 16 February 1990)
(Revised manuscript received 15 May 1990)

Key words: Anesthesia theory; Volatile anesthetic; Phospholipid bilayer; Lateral proton conductance; Impedance dispersion; Hydration layer

Impedance dispersion in liposomes measures the lateral charge transfer of lipid membrane surfaces. Depending on the choice of frequency between 1 kHz and 100 GHz, relaxation of the counterions at the interface, orientation of the head group, and relaxation of the bound and free water are revealed. This study measured the impedance dispersion in dipalmitoylphosphatidylcholine (DPPC) liposomes at 10 kHz. The surface conductance and capacitance showed breaks at pre- and main transition temperatures. Below the pre-transition temperature, the activation energy of the ion movement was 18.1 kJ · mol^{-1}, which corresponded to that of the spin-lattice relaxation time of water (18.0 kJ · mol^{-1}). At temperatures between pre- and main transition it increased to 51.3 kJ · mol^{-1}, and agreed with 46.2–58.0 kJ · mol^{-1} of the activation energy of the dielectric relaxation of ice. Because the present system was salt-free, the ions were H_3O^+ and OH^-, hence, their behavior represents that of water. The above results show that below the pre-transition temperature, the conductance is regulated by the mobility of free ions, or the number of free water molecules near the interface. On the other hand when the temperature exceeded pre-transition, melting of the surface-bound water crystals became the rate-limiting step for the proton flow. Halothane did not show any effect on the ion movement when the temperature was below pre-transition. When the temperature exceeded pre-transition, 0.35 mM halothane (equilibrium concentration) decreased the activation energy of the ion movement to 29.3 kJ · mol^{-1}. This decrease indicates that halothane enhanced the release of the surface-bound water molecules at pre-transition. The surface-disordering effect of halothane was also shown by depression of the pre-transition temperature and decrease of the association energy among head groups from 9.7 kJ · mol^{-1} of the control to 5.2 kJ · mol^{-1} at 0.35 mM.

Introduction

The frequency-dependent (1 kHz to 100 GHz) electrical impedance of aqueous suspension of phospholipid vesicles shows four dispersions. The impedance dispersions at about 1 kHz inform the relaxation of counterions near the vesicle membrane surfaces [1]. Those at 1 MHz inform the orientation of the hydrophilic head groups of the phospholipid molecules [2]. Those at 100 MHz and 10 GHz inform the relaxation of bound and free water molecules, respectively [3]. We [4] have reported that the temperature dependence of the surface capacitance and conductance parallel to the phospholipid membranes showed two peaks when the measuring frequency was below 120 Hz: at the pre-transition and the main phase transition temperatures. Thus, the lipid tail conformations and the interfacial properties are coupled.

The volatile anesthetics presently in clinical use are amphipathic due to the presence of 'acidic' protons in their molecular structure and tend to stay at the interface. The interfacial location of volatile anesthetics has been demonstrated by ^{1}H- and ^{19}F-NMR spectra of volatile anesthetics [5,6] where the hydrophilic end of the anesthetic molecules did not lose contact with the aqueous phase when bound to sodium dodecylsulfate micelles. Similar results were obtained with ^{19}F-NMR of halothane where the anesthetic showed tendency to saturate micellar surfaces [7]. A study with two-dimensional nuclear Overhauser effect proton-NMR [8] re-

Correspondence: T. Yoshida, Department of Applied Chemistry, Nagoya Institute of Technology, Showa-ku, Nagoya 466, Japan.

vealed that the cross-peak between methoxyflurane and dipalmitoylphosphatidylcholine (DPPC) vesicle membranes was observed only between the hydrophobic protons ($-CH_3$) of the anesthetic and the hydrophilic choline head protons ($-N(CH_3)_3$) of DPPC. The hydrophilic end of methoxyflurane stayed in the aqueous phase. Fourier transform infrared spectroscopy [9] showed that the interaction sites of volatile anesthetics on DPPC molecules were the phosphate moiety of the hydrophilic head and C=O moieties of the interfacial glycerol skeleton [10]. These data indicate the importance of the interfacial polar group of membranes and counterions in elucidating the mode of anesthetic actions.

This study measured the anesthetic effects on the temperature dependence of the electrical impedance of DPPC liposomes at 10 kHz. Because the system was salt-free, the obtained activation energies represent H_3O^+ and OH^-, and essentially the state of water. We shall analyze the proton flow and the head-group orientation at temperatures around the pre- and main transition.

Methods

1,2-Dihexadecanoyl-*sn*-glycero-3-phosphorylcholine (dipalmitoylphosphatidylcholine, DPPC) was obtained from Sigma, and thrice recrystallized from ethanol-water. DPPC was dried in vaccuo and mixed with water (DPPC/water, 1 : 9 w/w) in a tightly capped glass vial. The mixture was rigorously agitated in a flush mixer (Yamamoto, Tokyo) for 30 min at temperatures above the main phase transition. Halothane was obtained from Takeda (Osaka, Japan) and passed through activated aluminum oxide columns (Fluka) several times to remove water and the stabilizer (0.01% thymol). The anesthetic was added to the vesicle suspension by a microsyringe and the added amount was verified by weighing the glass vial. The capacitance and conductance were measured by an ac bridge (TR-IC, Ando Denki, Tokyo) at 10 kHz in a custom-built concentric cell made from platinum pipes. The cell volume was about 1.2 cm^3. The cell was immersed in a water bath and the temperature was controlled within 0.05 C° stability.

The phase transition of DPPC vesicles was measured by a differential scanning calorimeter (DSC 8230B, Rigaku Denki, Tokyo). The DPPC vesicle suspension was packed in an aluminum sample vial and closed airtight. The sample volume was 0.025 cm^3. The temperature was scanned at a rate of 1.0 C° per min between 10 and 60°C.

Experiments were repeated at least three times, and the data are expressed by the mean and standard error in Table I. Figures show typical runs. Because the scatters in the data were small, error bars were omitted for clarity.

Results and Discussion

The temperature effect on the conductance, G, and capacitance, C, of the DPPC vesicle suspension (DPPC/water, 10 : 90 w/w) is shown in Fig. 1. Both conductance and capacitance showed a break at about 33°C and 44°C. These values were close to the pre-transition (35°C) and the main transition temperature (42°C) obtained by differential scanning calorimetry. The temperatures were about two degrees lower for the pre-transition and about two degrees higher for the main transition. The cause of this difference is unclear. But it may be safe to assume that the conformational change of DPPC vesicles is coupled with the changes in the surface conductance and capacitance. The effects of various concentrations of halothane are shown in Figs. 2–4.

Schwarz [10] reported that the counterions move parallel to the membrane surface according to the externally applied electric field. The movements dissociate the center of gravity of cations and anions in their distribution, and the separation induces dipole mo-

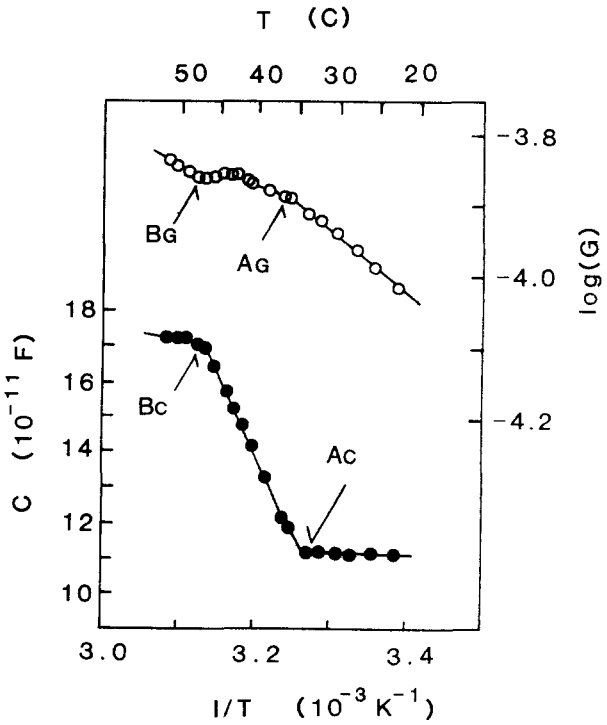

Fig. 1. The conductance (open circles) and capacitance (filled circles) measured at 10 kHz. A and B are the break points that correspond, respectively, to the pre- and main transition of DPPC vesicle membranes. Subscripts G and C signify conductance and capacitance, respectively. The temperatures for the break points in the impedance dispersion are slightly higher than the transition temperatures obtained by differential scanning calorimetry.

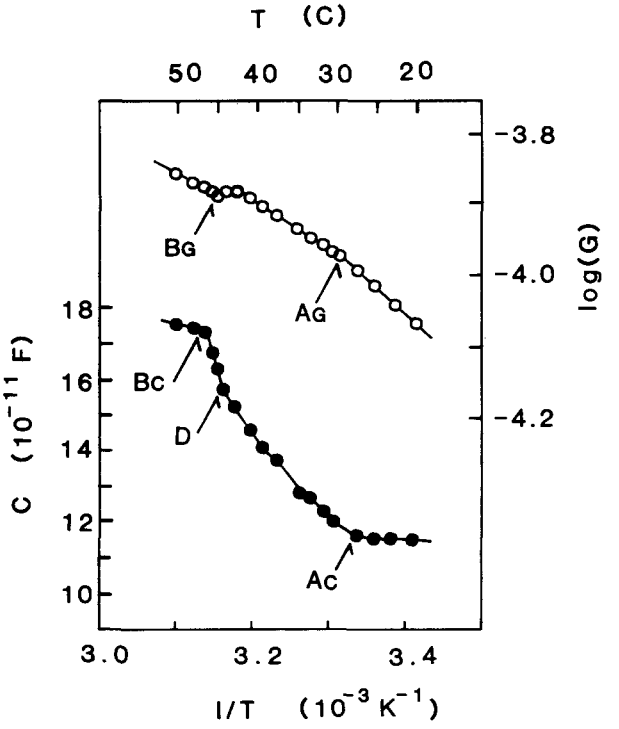

Fig. 2. Same as Fig. 1 in the presence of 4.2 mM halothane. A new break is observed at D. The D–B distance corresponds to the increased temperature span of the transition in the presence of volatile anesthetics.

ments. The static dielectric increment, $\Delta\epsilon$, generated by the induced dipole is expressed as

$$\Delta\epsilon = (9/4)\frac{p}{(1+p/2)^2}\frac{e^2rq}{\epsilon_r kT} \quad (1)$$

where q is the counterion surface density (ions per unit area), p the volume fraction occupied by the vesicle, r the radius of the vesicle, e the elementary charge, k the Boltzmann constant, ϵ_r the electrical permittivity near the vesicle surface, and T the absolute temperature.

The permanent dipole of the DPPC head group re-aligns under the applied external electric field, and adds dielectric increment to the system [2]. Schwan [1] reported, however, that this polarizing effect, induced by the headgroup orientation, was negligibly small compared to the counterion-induced polarizing effect. When the capacitance of the present vesicle suspension was measured at 1 MHz (not shown), the dip in the temperature effect disappeared. The capacitance remained constant in the total temperature range with the values of about $6.4 \cdot 10^{-11}$ to $6.9 \cdot 10^{-11}$ F. The temperature effect at 1 MHz represents mainly the polarization induced by the head-group alignment [1]. Hence, the effect of the head-group alignment on the temperature profile of the impedance of the present system may be negligibly small. The capacitance change in Fig. 1 is attributable mainly to the induced polarization by counterion distribution.

A. Temperatures below the pre-transition

At this low temperature range, the capacitance in Fig. 1 showed a constant value. This implies that the surface density of the counterion, q, stayed almost constant during the temperature elevation. At temperatures below the pre-transition, the zwitterionic dipole of the DPPC head groups is aligned parallel to the membrane surface [11–14]. The intermolecular interactions between the head groups appear to be undisturbed until the temperature exceeds pre-transition. The charge density of the vesicle surface stayed constant, and, therefore, the counterion surface concentration did not change.

The number of free ions in a unit volume is expressed by n_f, its mobility by μ. Assuming that the conductance, G, of the liposome is mainly determined by the free ions in the aqueous phase, G is expressed as

$$G = A \cdot e \cdot n_f \cdot \mu \quad (2)$$

where A is the cell constant, and e is the electron charge of the ion.

The free ions in the bulk aqueous solution are in a dynamic equilibrium with the bound ions at the vesicle surface. At equilibrium, the adsorption velocity of the ion equals the desorption velocity, and

$$k_a n_f (n_s - n_a) = k_d n_a \quad (3)$$

where k_a and k_d are the adsorption and desorption rate constants, respectively, and n_a and n_s are the number of ions adsorbed onto a unit vesicle surface and the number of adsorption sites, respectively. When the concentration of the ion is dilute, it may be assumed that $n_s > n_a$. The total number of ions, n_t, in the system is $n_t = n_a + n_f$. Eqn. 3 is rewritten as

$$k_a n_f n_s = k_d (n_t - n_f) \quad (4)$$

or

$$n_f = \frac{n_t}{(k_a/k_d)n_s + 1} \quad (5)$$

Because $(k_a/k_d) \gg 1$, Eqn. 5 can be approximated as

$$n_f = (k_d/k_a)(n_t/n_s) \quad (6)$$

As discussed above, the intermolecular interaction among DPPC head groups remains unchanged at temperatures below the pre-transition. Also, the surface density of the fixed charges does not change. Then, the number of the adsorption site, n_s, is constant so that

the number of the free ions, n_f, is constant according Eqn. 6. This number of the free ions is expressed by n_0.

The mobility of the free ion, μ, is expressed by the activation law as follows.

$$\mu = \mu_0 \exp(-\epsilon_\mu / kT) \tag{7}$$

From Eqn. 7 and the condition of $n_f = n_0$, Eqn. 2 is expressed in a logarithmic form.

$$\log G = (-\epsilon_\mu / 2.3k)(1/T) + \text{constant} \tag{8}$$

Eqn. 8 expresses the effects of temperature on G below the pre-transition. From the plot between log G and $1/T$ in Fig. 1 at temperatures below the pre-transition, the activation energy for the ion mobility, $-\epsilon_\mu$, was estimated to be 18.1 kJ/mol. This value corresponds to the activation energy of water (18.0 ± 0.3 kJ · mol^{-1}) obtained by the spin-lattice relaxation times of proton NMR [15]. These data indicate that the conductance is mainly regulated by the mobility of free ions (H_3O^+ and OH^-) at this temperature range, and support the proposed model.

B. Temperatures between pretransition and main transition

When the temperature reaches pre-transition, the intermolecular interactions between DPPC head groups start to weaken. As a result, the degree of freedom of the head-group motion increases [2,16] and so does the surface density of the fixed charges. This is equivalent to the increase in the number of the adsorption sites at the surface, n_s, for the free-ion. By designating ϵ_n for the association energy between DPPC head groups, n_s is expressed as

$$n_s = B \exp(-\epsilon_n / kT) \tag{9}$$

From Eqns. 6 and 9

$$n_f = B^{-1}(k_d / k_a) n_t \exp(\epsilon_n / kT) \tag{10}$$

By assuming k_d/k_a is nearly constant at a short temperature range between pre-transition and main transition, it follows

$$n_f = B' \exp(\epsilon_n / kT) \tag{11}$$

From Eqns. 2, 7 and 11,

$$\log G = \{(\epsilon_n - \epsilon_\mu)/2.3k\}(1/T) + \text{constant} \tag{12}$$

From the slope of the plot between log G and $1/T$ in the temperature range between the pre-transition and main transition (about 42°C, below the dip), the value for $\epsilon_n - \epsilon_\mu$ is obtained. By combining the ϵ_μ value estimated in the preceding section, ϵ_n was found to be 9.7 kJ · mol^{-1}.

The excess enthalpy of pre-transition of DPPC vesicles, estimated by differential scanning calorimetry, is 7.7 to 9.7 kJ · mol^{-1} [17,18]. This enthalpy change is related to the energy increase induced by the increased motion of the DPPC head group, and matches the above ϵ_n value. This agreement supports our model that the number of the free ions decreases at temperatures above the pre-transition level by the enhanced adsorption of the counterions onto the increased binding sites on the DPPC surfaces.

We assume that the mobility, μ', of the counterion, which is bound to the vesicle surface, is different from the mobility of the free-ion, and is expressed by the following equation [19].

$$\mu' = \mu'_0 \exp(-\epsilon'_\mu / kT) \tag{13}$$

From Eqns. 3. 6, and 9, and from the condition $1/n_t \approx 0$

$$n_a = n_s = B \exp(-\epsilon_n / kT) \tag{14}$$

The term q in Eqn. 1 is the number of counterions that are mobile under the external electrical field. In the present system, q is variable. It depends on temperature and is proportional to $\mu' \cdot n_a$. Hence, $\Delta\epsilon$ in Eqn. 1 is proportional to $\mu' n_a / T$. On the other hand, the capacitance measured at 10 kHz is comprised of three parts: contributions from the surface-bound counterion, DPPC head groups, and water [1,2]. Let ΔC be $C - C(1\text{ MHz})$, then, ΔC represents the contribution from the counterion only. Because ΔC is proportional to $\Delta\epsilon$ in Eqn. 1,

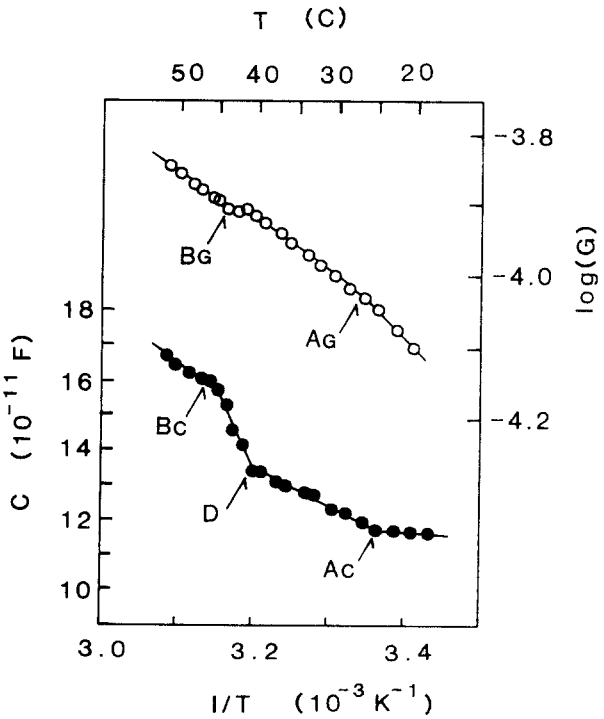

Fig. 3. Same as Fig. 1 in the presence of 8.8 mM halothane.

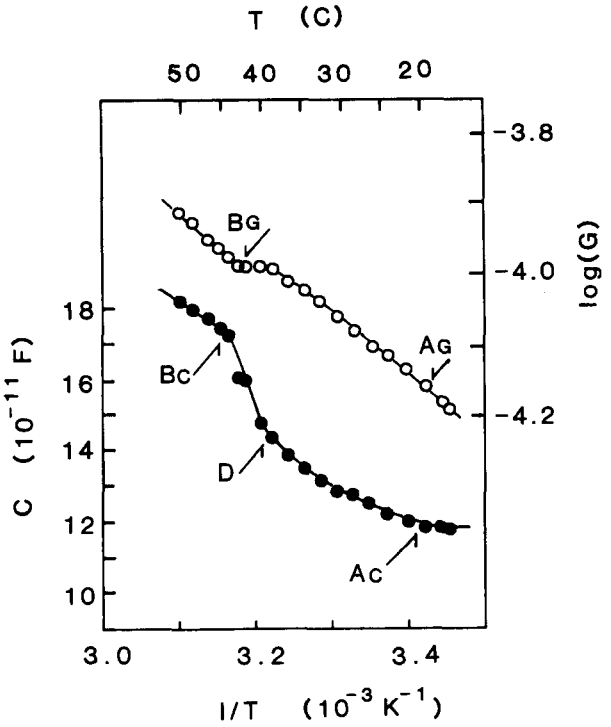

Fig. 4. Same as Fig. 1 in the presence of 12.8 mM halothane.

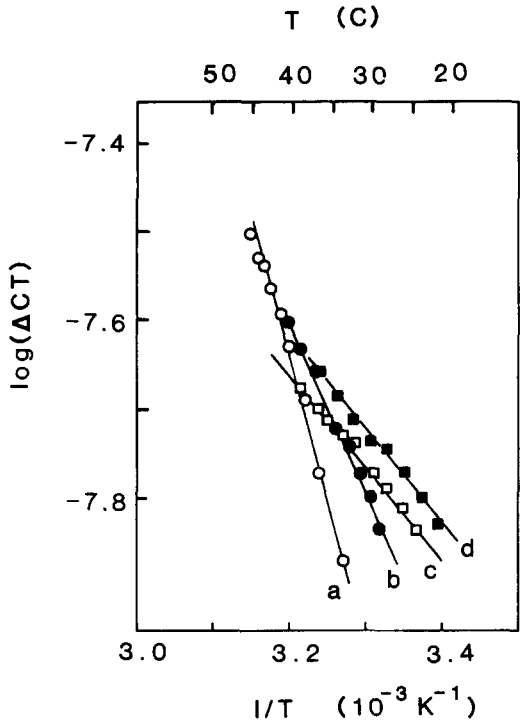

Fig. 5. The Arrhenius plot of the counterion-dependent capacitance between pre- and main transition temperatures. a, Control; b, halothane 4.2 mM; c, 8.8 mM, and d, 12.8 mM.

the following relation is derived from Eqns. 1, 13 and 14.

$$\log(T\Delta C) = \{(-\epsilon_n - \epsilon'_\mu)/2.3k\}(1+T) + \text{constant} \quad (15)$$

Fig. 5 shows the plot of $\log(T\Delta C)$ versus $1/T$ at the temperatures between the pre-transition and the main transition. From the slope of this plot, $\epsilon_n + \epsilon'_\mu$ is obtained according to Eqn. 15. From this value and ϵ_n, estimated from the temperature dependence of the conductance, ϵ'_μ was found to be 51.3 kJ · mol^{-1} (Table I). This value is much larger than the ϵ_μ (18.1 kJ · mol^{-1}) of the free ion in Section A. The mobile ions in the present system are H_3O^+ and OH^- ions and are responsible for the anomalous conduction involving the formation and disruption of hydrogen bonds. The mobility of the water molecules bound to the vesicle surface is restricted, hence $\epsilon'_\mu > \epsilon_\mu$. This relation is analogous to the freezing of water where the decrease of degree of freedom increases the activation energy of the dielectric relaxation to 46.2–58.0 kJ · mol^{-1} [20]. When one accepts the concept that the surface-bound water molecules are structured with stabilized hydrogen bonds and ice-like, the estimated 51.3 kJ · mol^{-1} for ϵ'_μ is a reasonable value.

C. Temperature above the main transition

The temperature profile of conductance G exhibited a small dip at the point marked B_G (Fig. 1). This temperature agrees with the main-transition temperature obtained by differential scanning calorimetry (Fig. 6). The melting of DPPC hydrocarbon chains and the increased thermal fluctuation affects the head-group motion. Together with the lateral membrane expansion at the main transition, that increases head-group distances, the increased head-group motion would disrupt the linkage between head groups. This separation of the intermolecular linkages between head groups creates additional surface charges and decreases the free-ion concentrations. Because melting of hydrocarbon chains occurs in a small temperature span, the free-ion concentration decreases abruptly. This steep decrease in n_f would overcome the temperature-induced increase in

Table I

The activation energies estimated by the temperature dependence of conductance and capacitance of the dipalmitoylphosphatidylcholine liposome

Values of ϵ are presented as means ± S.E. ($n = 3$). ϵ_μ: The Arrhenius activation energy of free-ion mobility. ϵ_n: The Arrhenius activation energy of association among solid-gel DPPC head groups. ϵ'_μ: The Arrhenius activation energy of bound-ion mobility. $\epsilon_n(h)$: The Arrhenius activation energy of association among liquid-crystalline DPPC head groups.

Halothane (mM)	ϵ_μ	ϵ_n	ϵ'_μ	$\epsilon_n(h)$
0	18.1 ± 0.3	9.7 ± 0.6	51.3 ± 1.0	5.8 ± 0.6
4.2	17.8 ± 0.3	5.2 ± 0.8	29.3 ± 1.0	5.9 ± 0.6
8.8	18.1 ± 0.3	3.1 ± 0.8	17.3 ± 1.0	2.7 ± 0.6
12.8	18.0 ± 0.4	3.0 ± 0.8	17.9 ± 1.0	1.8 ± 0.8

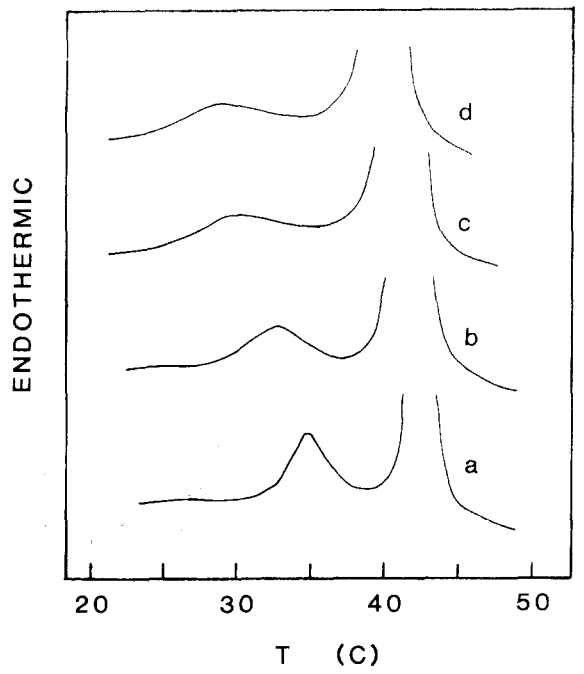

Fig. 6. DSC scan of the DPPC vesicles. a, Control; b, halothane 4.2 mM; c, 8.8 mM, and d, 12.8 mM.

the ion mobility. As a net result, the conductance decreases according to Eqn. 2. Further increase in temperature lets the thermally-induced ion mobility to dominate, and the conductance starts to increase again. This sequence forms the temporary minimum in the temperature profile of the conductance.

If the conductance is regulated by the temperature effect on the ion mobility alone, Eqn. 8 will hold as in Section A. When the slope of the plot between log G versus $1/T$ at temperatures above B_G was used to calculate ϵ_μ, the value was about 1/3 of ϵ_μ found in Section A. This underestimation apparently originates from the omission of the possible decrease in the number of free ions, n_f. Hence, Eqn. 12 was used in this high temperature range as described in Section B to estimate $\epsilon_n - \epsilon_\mu$. If the conductance is assumed to be controlled mainly by free ions, the ϵ_μ values in the high temperature range should be equal to those estimated in Section A in the low temperature range. By combining the $\epsilon_n - \epsilon_\mu$ value obtained by Eqn. 12 and the ϵ_μ value in Section A, ϵ_n in the high temperature range, $\epsilon_n(h)$, was estimated to be 5.8 ± 0.5 kJ · mol^{-1}. The value was about 1/2 of the ϵ_n value found in Section B for the solid-gel membrane. This difference in ϵ_n values suggests that the mobility of the DPPC head groups is increased in the liquid-crystalline phase and the linkage between head groups can be broken with about 1/2 energy compared to the solid-gel phase.

Effect of halothane

Figs. 2–4 show the effect of halothane (4.2, 8.8, and 12.8 mM) on the temperature profile of the conductance and capacitance of the vesicle suspension. There appears to be a general misunderstanding about bulk anesthetic (or any other drugs) concentrations. Drug concentrations are traditionally expressed by mM unit in a test solution, as in the present article. The distribution of drugs, however, is not uniform between aqueous phase and the organic phase, such as proteins or membranes. Despite the tendency to compare the drug potencies by the bulk concentration, it does not represent the drug activity. This problem has already been dealt with by Ferguson [21] more than 50 years ago. Nevertheless, because an anonymous referee of this article questioned the validity of this work on the ground that the anesthetic concentrations were too high, an annotation on bulk drug concentration is in order.

In this study, DPPC was mixed with water at 1 : 9 w/w. Let the number of halothane molecules added to the system be expressed by A. After partition into the lipid membrane, the number of remaining anesthetic molecules in water is expressed by x. Then, the number of anesthetic molecules bound to DPPC becomes $A-x$. The molality partition coefficient of halothane between DPPC and water is about 98.5 [22,23]. Then,

$$98.5 = (A-x)/(x/9) \quad \text{hence,} \quad x = 0.08372 \cdot A \tag{16}$$

The total concentrations of 12.8, 8.8, and 4.2 translate into about 1.07, 0.73, and 0.35 mM (equilibrium aqueous concentrations), respectively. The blood concentration varies with the protein content, Ht, etc. It also varies with the tissue; blood or brain. The so-called clinical concentrations of volatile anesthetics (EC_{50}) expressed in mM have little meaning. This is one of the reasons that the MAC (minimal alveolar concentrations) concept was evolved. MAC is expressed by the partial pressure of the anesthetics in the gas phase in equilibrium with the reaction mixture. Using Ostwald solubility coefficient of halothane to water, the above anesthetic concentrations are equivalent to $3.06 \cdot 10^{-2}$, $2.09 \cdot 10^{-2}$, and $1.00 \cdot 10^{-2}$ atm, respectively, in the gas phase.

A larger change was seen in the capacitance. The break point of the capacitance, A_C, was shifted to lower temperatures and a new break appeared at point D. The break point of the conductance, A_G, was also shifted to the lower temperatures corresponding to the change in A_C. These temperatures agree with the pre-transition temperature obtained by differential scanning calorimetry (Fig. 6). Accordingly, ϵ_μ values of the halothane-doped DPPC were estimated by Eqn. 8. Halothane did not affect ϵ_μ values appreciably (Table I). Because ϵ_μ is the parameter related to the mobility of free ions, this insignificant effect of halothane is not unreasonable.

The new break at point D appears to relate to the increase of the temperature span of the phase transition by volatile anesthetics. It has been known that volatile

anesthetics increase the width of the main transition [24–26]. Figs. 2–4 show that the main phase-transition starts at D and continues to B_C. Point B_C indicates the end of the transition. In the presence of 12.8 mM halothane, the width of the main transition was about 6 C°. The figure suggests that the pre-transition also widens and occupies the temperature range from A to D.

The temperature dependence of the capacitance ΔC, was estimated by Eqn. 15 from the slope of the capacitances between A_C and D (Fig. 5). From the slope of this figure, the values for $\epsilon_n + \epsilon'_\mu$ in the presence of halothane were obtained. The ϵ_n values were obtained by Eqn. 12 from the temperature-dependence of the conductance. From the difference between these two, the ϵ'_μ values were estimated to be 29.3, 17.3, and 17.9 $kJ \cdot mol^{-1}$ for 4.2, 8.8, and 12.8 mM halothane, respectively (Table I).

Halothane decreased both ϵ_n and ϵ'_μ. When halothane molecules are adsorbed onto the vesicle surface, the hydrogen bonds among the surface-bound water molecules are broken [27–30], and the degree of freedom of the motion of water molecules increases. The decrease in order at the interfacial region enhances the mobility of the DPPC head groups, resulting in the decrease in the interaction energy, ϵ_n, among head groups. The result that ϵ_n values are similar between the system with halothane 8.8 and 12.8 mM suggests that the halothane concentration at the surface approached a saturation level. The increase in the degree of freedom of the surface-bound water molecules would increase the mobility of H_3O^+ and OH^- ions parallel to the membrane surface, and decreases the ϵ'_μ values.

The slopes of capacitance between points D and B_C (Figs. 2–4) are about equal to the control between A_C and B_C in Fig. 1. When the membrane is thermally transformed into the liquid-crystalline state, the head-group motion increases. Because the state of the interfacial region of the liquid-crystalline membrane is already disordered similar to the anesthetic-doped membrane, the anesthetic effect becomes marginal.

From the conductance at temperatures above B_G, $\epsilon_n(h)$ was estimated by Eqn. 12. The value in the presence of 4.2 mM halothane was the same as $\epsilon_n(h)$ of the control. When the halothane concentration was increased to 8.8 and 12.8 mM, however, the values dropped to about half of the control. This result suggests that the high concentration of halothane increased the thermal motion of the DPPC lipid tails.

The halothane action changes between 4.2 and 8.8 mM (Table I). From a study on planar lipid bilayer membranes, we have shown [31] that halothane interacted with a planar lipid bilayer with saturation kinetics when the concentration was below 5.4 mM. When halothane concentration exceeded this level, nonsaturable interaction occurred. Similar concentration-dependent difference in the anesthetic action was also noted from the present data (Table I). The values of ϵ_n and ϵ'_μ started to saturate when the halothane concentration exceeded 4.2 mM. Presumably, $\epsilon_n(h)$ is related to the thermal motion of the lipid tails, and halothane may enhance the tail melting at high concentrations. By proton NMR, Shieh et al. [32] and Yokono et al. [33] reported differential effects of volatile anesthetics on the motions of choline head and lipid tails. They showed that anesthetic-induced isothermal phase transition of DPPC vesicle membranes occurred in two stages. At subclinical anesthetic concentrations, the signals only from choline protons appeared in the frequency domain. The signals from the lipid tail protons appeared when the anesthetic concentration was increased.

The primary effect of halothane appears to be the increase in the motion of the head group of the phospholipid vesicles rather than the hydrocarbon chain. The anesthetic increased the movement of H_3O^+ and OH^- ions parallel to the vesicle surfaces. This result indicates that the surface-bound water molecules are mobilized and agrees with the Fourier transform infrared study of DPPC in water-in-oil reversed micellar system reported by Tsai et al. [9]. They found that the free O–H stretching band of unbound water increased when volatile anesthetics were added, showing that the anesthetics released the water molecules, that bound to DPPC, into the bulk aqueous phase.

Acknowledgments

Supported in part by the VA Medical Research, and NIH grants GM25716 and GM27670.

References

1 Schwan, H.P., Takashima, S., Miyamoto, V.K. and Stoekenius, W. (1970) Biophys. J. 10, 1102–1119.
2 Shepherd, J.C.W. and Büldt, G. (1978) Biochim. Biophys. Acta 514, 83–94.
3 Kaatze, U., Henze, R., Seegers, A. and Pottel, R. (1975) Ber. Bunsenges. Physik. Chem. 79, 42–53.
4 Yoshida, T., Taga, K., Okabayashi, H., Kamaya, H. and Ueda I. (1989) Biochim. Biophys. Acta 984, 253–256.
5 Kaneshina, S., Lin, H.C. and Ueda, I. (1981) Biochim. Biophys. Acta 647, 223–226.
6 Yoshida, T., Takahashi, K. and Ueda, I. (1989) Biochim. Biophys. Acta 985, 331–333.
7 Yoshida, T., Takahashi, K., Kamaya, H. and Ueda, I. (1988) J. Colloid Interface Sci. 124, 177–185.
8 Yokono, S., Ogli, K., Miura, S. and Ueda, I. (1989) Biochim. Biophys. Acta 982, 300–302.
9 Tsai, Y.S., Ma, S.M., Kamaya, H. and Ueda, I. (1987) Mol. Pharmacol. 31, 623–630.
10 Schwarz, G. (1962) J. Phys. Chem. 66, 2636–2642.
11 Büldt, G. and Wohlgemuth, R. (1981) J. Membr. Biol. 58, 81–100.
12 Seelig, J., Gally, H.U. and Wohlgemuth, R. (1977) Biochim. Biophys. Acta 467, 109–119.
13 Hauser, H., Guyer, W., Pascher, I., Skrabal, P. and Sundell, S. (1980) Biochemistry 19, 366–373.

14 Yeagle, P., Hutton, W.C., Huang, C. and Martin, R.B. (1975) Proc. Natl. Acad. Sci. USA 72, 3477–3481.
15 Yoshino, A., Yoshida, T. and Takahashi, K. (1989) Magn. Res. Chem. 27, 344–347.
16 Mashimo, T., Ueda, I., Shieh, D.D., Kamaya, H. and Eyring, H. (1979) Proc. Natl. Acad. Sci. USA 76, 5114–5118.
17 Janiak, M.J., Small, D.M. and Shipley, G.G. (1976) Biochemistry 15, 4575–4580.
18 Hinz, H.J. and Sturtevant, J.M. (1972) J. Biol. Chem. 247, 6071–6075.
19 Pethig, R. (1979) Dielectric and electronic properties of biological materials, p. 172, Wiley, New York.
20 Pethig, R. (1979) Dielectric and electronic properties of biological materials, p. 139, Wiley, New York.
21 Ferguson, J. (1939) J. Proc. Roy. Soc. London B. 127, 387–404.
22 Kamaya, H., Kaneshina, S. and Ueda, I. (1981) Biochim. Biophys. Acta 646, 135–142.
23 Simon, S.A., McIntosh, T.J., Bennet, P.B. and Shrivastav, B.B. (1979) Mol. Pharmacol. 16, 163–170.
24 Jain, M.K. and Wu, N.M. (1977) J. Membr. Biol. 34, 157–201.
25 Mountcastle, D.B., Biltonen, R.L. and Halsey, M.J. (1978) Proc. Natl. Acad. Sci. USA 75, 4906–4910.
26 Kaminoh, Y., Tashiro, C., Kamaya, H. and Ueda, I. (1988) Biochim. Biophys. Acta 946, 215–220.
27 Di Paolo, T. and Sandorfy, C. (1974) J. Med. Chem. 17, 809–814.
28 Trudeau, T., Dumas, J.-M., Dupuis, P., Guerin, M. and Sandorfy, C. (1980) Topics Curr. Chem. 93, 91–125.
29 Hobza, P., Mulder, F. and Sandorfy, C. (1981) J. Am. Chem. Soc. 103, 1360–1366.
30 Hobza, P., Mulder, F. and Sandorfy, C. (1982) J. Am. Chem. Soc. 104, 925–928.
31 Yoshida, T., Mori, T. and Ueda, I. (1983) J. Colloid Interface Sci. 96, 39–47.
32 Shieh, D.D., Ueda, I., Lin, H.C. and Eyring, H. (1976) Proc. Natl. Acad. Sci. USA 73, 3999–4002.
33 Yokono, S., Shieh, D.D. and Ueda, I. (1981) Biochim. Biophys. Acta 645, 237–242.